7282 *Macromolecules* **1993,** *26,* 7282–7287

Conformationally Induced Localization in the Electronic Structure of Polysilanes

J. V. Ortiz*

Department of Chemistry, University of New Mexico, Albuquerque, New Mexico 87131-2609

Celeste McMichael Rohlfing

Theoretical Division, Sandia National Laboratories, Livermore, California 94551-0969

Received April 15, 1993; Revised Manuscript Received October 5, 1993[●]

ABSTRACT: *Ab initio* electron propagator calculations with a double ζ effective core potential basis on the vertical electron binding energies of oligomeric models of polysilane chains reveal the effects of gauche conformational defects on electronic structure. When a gauche defect lies between two all-trans segments of unequal lengths, most of the probability density for the Feynman–Dyson amplitudes corresponding to the lowest ionization energy or the largest electron affinity resides on the longer segment. The energy gap between cationic and anionic states increases when a gauche defect is introduced, but the effect is larger when the defect is in the middle of the chain. These trends are explained in terms of simple bond function models suggested by examination of the Feynman–Dyson amplitudes.

Introduction

Polysilanes, saturated chains with backbones composed of silicon atoms, possess a variety of interesting spectroscopic, optical, photochemical, and structural properties.[1,2] Despite their lack of double bonds, lone pairs and d electrons, these molecules exhibit large oscillator strengths in the near ultraviolet.[3] Abrupt red shifts upon cooling[4] have been attributed to coil-to-rod transformations and to shorter range conformational changes.[5] Increases in pressure may produce red-shifts that are sometimes followed by blue shifts at higher pressures.[6] Changes in conformations, bond angles and bond lengths in the silicon backbone generally are held to be responsible for these and other effects. Photochemical decomposition of polysilanes in thin films and in solution involves silylene and other radical intermediates.[7] Observations of photoconductivity[8] have stimulated interest in using polysilanes as self-developing photoresists.[9] In addition, these materials are convenient synthetic precursors to silicon carbide materials.[10]

The electronic structure of saturated silicon chains underlies these phenomena and their applications. Calculations on model (generally hydrogen-substituted) oligomers with *ab initio*[11–17] and semiempirical methods[18–20] have determined equilibrium structures, rotation barriers, vibrational frequencies, and other parameters characterizing the ground state potential energy surface. Recent oligomer calculations have considered polarizabilities as well.[21] Studies of infinite polymers with translational symmetry have yielded analogous ground state information and have provided band structures as well.[22–26] From results on ionic[11–15] and excited states[27,28] of oligomers, it is clear that rotations about Si–Si single bonds from trans to gauche conformations produce higher ionization energies, more negative electron affinities and larger excitation energies. In-phase relationships between non-neighbor Si–Si bond functions grow in importance in gauche conformations, stabilizing occupied one-electron levels and causing higher ionization energies. At the same time, out-of-phase relationships between non-neighbor Si–Si functions with σ antibonding and π bonding character destabilize unoccupied one-electron levels, producing smaller electron affinities. This widening of the gap one-electron levels implies larger excitation energies.

A central question that emerges from these experimental and theoretical studies pertains to the nature of the chromophores responsible for many of the properties discussed above. Such a characterization is needed for judging the relevance of certain models of coil-to-rod transitions that assume localized excitations.[29] A recent semiempirical calculation[27] on $Si_{20}H_{42}$ suggests that introduction of gauche conformational defects in otherwise trans chains leads to independent chromophores confined to trans segments separated by the defects. In calculations on all-trans chains, the highest occupied molecular orbital has its largest absolute amplitudes near the center of the chain; a gradual decline toward the ends of the chains also is obtained. Upon introduction of a gauche defect, the absolute amplitudes increase on the longer of the two trans segments separated by the rotated bond, while the absolute amplitudes sharply decrease on the shorter trans segment. While this trend is quite pronounced for the highest occupied molecular orbital, there is no such effect for the lowest unoccupied molecular orbital in these calculations. Certain experimental results also suggest the possibility of conformationally separated chromophores. Recent photophysical measurements on $Si_{16}(CH_3)_{34}$ in solution and in glasses have shown close similarity to typical polymers.[30] The model employed to explain the spectra asserts that a statistical collection of all-trans chain segments absorbs at various frequencies and that emission occurs from the chromophore with the lowest possible excitation energy, an all-trans segment that is 16 silicons long. Lifetime measurements on oligomers with silicon backbones of different lengths[31] and transient absorption experiments[32] suggest that the chromophores present in polymers are between 10 and 15 silicons long. An alternative view is based on band calculations[33] in which gauche conformations are introduced in otherwise all-trans unit cells of several sizes. No localization of states in trans or gauche regions emerges from these results. Localization obtained in earlier oligomer calculations[27] is held to originate in approximations inherent in the semiempirical method.[33] Symmetry restraints are inherent in the band calculations and may themselves introduce artefacts that are not applicable to polymers.

[●] Abstract published in *Advance ACS Abstracts*, November 15, 1993.

0024-9297/93/2226-7282$04.00/0

To deepen understanding of polysilane chromophores, *ab initio* electron propagator calculations are undertaken presently. The methods employed below have been demonstrated to yield accurate ionization energies and ground state energies for small oligomers.[14] They are applied to oligomers with six to ten silicons, the smallest chains in which localization in all-trans segments of different lengths could be obtained. Symmetry's role is examined by studying oligomers with gauche conformational defects in different positions.

Methods

Orbital energies and two-electron integrals in the canonical orbital basis are produced by Gaussian 90.[34] This information is required by the electron propagator program EPT90[35] for the calculation of electron binding energies and Feynman–Dyson amplitudes. Gaussian 90 also calculates second order many-body perturbation theory[36] total energies. Effective core potentials (ECP's) for Si[37] eliminate explicit consideration of the Si 1s, 2s, and 2p electrons. Because of their success in calculations on oligomers up to Si_5H_{12},[14] double ζ basis sets for Si[37] and H[38] are used. In extensive studies of various approximations involving basis sets, ECP's and correlation methods, it was found that excellent agreement with experiment is obtained.[14] This agreement is partly due to cancellations of errors pertaining to the ECP orbital energies (+0.1 eV), reduced basis correlation corrections (+0.1 eV), and the deficiencies of partial fourth order propagator self-energies (−0.2 eV). The present methods represent the best compromise of accuracy and efficiency that is feasible for the longer chains presently under consideration.

Geometries of the silane oligomers are defined by parameters that were optimized in previous studies on shorter chains with larger basis sets.[11,13] Si–Si and Si–H bond lengths are 2.345 and 1.481 Å, respectively. Values of 110 and 109.471° define Si–Si–Si and Si–Si–H bond angles, respectively. Calculations on chains of various lengths in different conformations have shown that these parameters vary little from the values above when they are optimized.[11,13] Dihedral angles defined by four contiguous Si's in the all-trans chains are 180°. When a gauche rotational defect is introduced, one of these dihedral angles becomes 60°. The notation X-Y, where X and Y are integers labeling Si atoms, denotes the position of the Si–Si bond where rotation to the gauche conformation has taken place. For example, in the 4–5 gauche conformer, the plane defined by Si atoms 3, 4, and 5 is rotated 60° with respect to the plane of Si atoms 4, 5, and 6.

Electron propagator theory (EPT)[39] produces vertical electron binding energies (ionization energies and electron affinities) and corresponding Feynman–Dyson amplitudes. Propagator electron binding energies contain relaxation and correlation corrections to Koopmans' theorem[40] values, the negatives of canonical orbital energies. To every ionization energy, there corresponds a Feynman–Dyson amplitude (FDA)

$$\int \Psi^{*}_{N-1}(x_2,x_3,x_4,\ldots,x_N)\Psi_N(x_1,x_2,x_3,\ldots,x_N)\,dx_2\,dx_3\,dx_4\ldots dx_N = \phi^{\mathrm{FDA}}(x_1)$$

where the initial state has N electrons. Because it is a function of the space-spin coordinates of a single electron, the FDA is a spin-orbital. Each ionization energy or electron affinity corresponds to an FDA just as an energy corresponds to each canonical molecular orbital. Hartree–Fock theory defines the zeroth order propagator matrix, $\mathbf{G}_0(E)$, where

$$\{\mathbf{G}_0^{-1}(E)\}_{ij} = (E - \epsilon_i)\delta_{ij}$$

and ϵ_i is the ith canonical orbital energy. Several approximate self-energy matrices, $\boldsymbol{\Sigma}(E)$, provide relaxation and correlation corrections in the solution of the Dyson equation,

$$\mathbf{G}^{-1}(E) = \mathbf{G}_0^{-1}(E) - \boldsymbol{\Sigma}(E)$$

where one seeks E such that

$$\det\{\mathbf{G}^{-1}(E)\} = 0$$

Table I. All-Trans Total Energies (au) and Electron Binding Energies (eV)

molecule	HF	MBPT(2)	Koopmans	EPT(2)	EPT(P4)
Si_6H_{14}	−30.577 87	−30.890 28	9.48	8.58	8.74
			−2.67	−1.90	−1.99
Si_7H_{16}	−35.484 94	−35.848 46	9.32	8.39	8.56
			−2.51	−1.71	−1.80
Si_8H_{18}	−40.392 01	−40.806 64	9.19	8.25	8.42
			−2.40	−1.57	−1.66
Si_9H_{20}	−45.299 09	−45.764 82	9.10	8.14	8.31
			−2.30	−1.46	−1.55
$Si_{10}H_{22}$	−50.206 16	−50.723 00	9.02	8.05	8.23
			−2.23	−1.37	−1.46

In previous studies,[14] second order, third order, and partial fourth (P4) order[41] self-energies have been applied to smaller chains with larger basis sets. These results demonstrated that second order corrects most of the errors made by Koopmans' theorem and that partial fourth order theory provides fine improvements over second order. Neglect of off-diagonal terms in the self-energy matrix has little effect on electron binding energies or FDAs. The diagonal self-energy approximation yields an FDA which is equal to a canonical orbital, but with an electron binding energy that includes electron correlation. Calculations of this type with the basis sets described above provide an accurate description of photoelectron spectra[14,42] (agreement within 0.1 eV obtains for short oligomers) and are feasible for longer chains.

Results

Calculations on trans chains from six to ten Si atoms yield the results of Table 1. In the last three columns, negative electron binding energies are listed. Thus, positive numbers are ionization energies and negative numbers are electron affinities. (Anions are not bound in this model.) With increasing chain length, ionization energies decline and electron affinities become less negative. Most of the correlation corrections occur in second order (EPT(2)); additional corrections are smaller than 0.2 eV. Propagator ionization energies are smaller than Koopmans' theorem[40] results; orbital relaxation in the cationic states is the likely cause of this effect. Correlated electron affinities, however, are larger than their uncorrelated counterparts, indicative of greater correlation effects in the anions than in the neutrals. Second order calculations tend to exaggerate the corrections to Koopmans' theorem values; higher order calculations are generally intermediate between the two.[39]

Results on chains with one gauche single bond are presented in Table 2. Beneath each molecule in the first column is the X–Y position of the rotated bond. These positions have been chosen in order to study situations in which the remaining all-trans fragments have the greatest lengths possible. Chains with odd numbers of Si atoms have no symmetry operations when such a rotation is performed. When the central Si–Si bond of a chain with

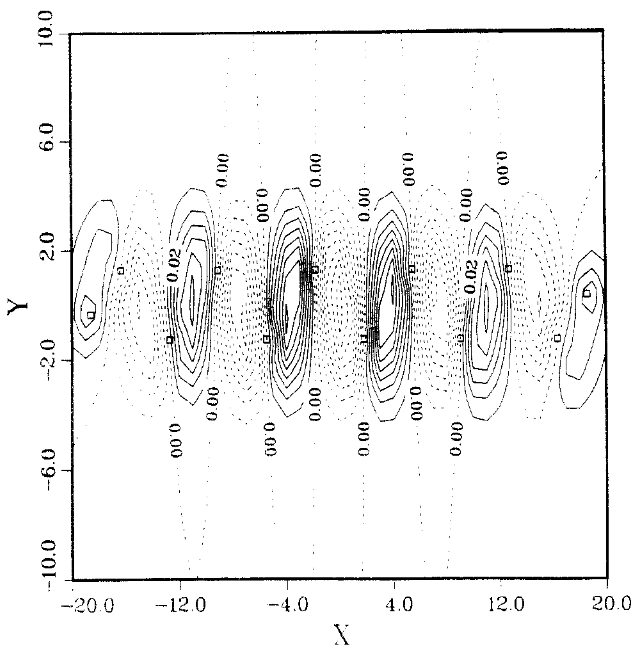

Figure 1. Feynman–Dyson amplitude for the ionization energy of $Si_{10}H_{22}$.

Table II. Gauche Total Energies (au) and Electron Binding Energies (eV)

molecule	HF	MBPT(2)	Koopmans	EPT(2)	EPT(P4)
Si_7H_{16}	-35.484 56	-35.848 53	9.60	8.66	8.84
3-4			-2.78	-1.98	-2.07
Si_8H_{18}	-40.391 65	-40.806 75	9.49	8.54	8.72
4-5			-2.70	-1.88	-1.97
Si_8H_{18}	-40.391 62	-40.806 71	9.43	8.48	8.66
3-4			-2.60	-1.77	-1.87
Si_9H_{20}	-45.298 71	-45.764 93	9.37	8.41	8.59
4-5			-2.58	-1.73	-1.83
$Si_{10}H_{22}$	-50.205 77	-50.723 11	9.30	8.33	8.51
5-6			-2.53	-1.67	-1.76
$Si_{10}H_{22}$	-50.205 79	-50.723 12	9.26	8.28	8.46
4-5			-2.45	-1.59	-1.69

an even number of Si atoms is rotated, the gauche isomer retains a C_2 symmetry operation and the FDAs will have **a** or **b** labels. Such classifications do not apply to chains where the rotated bond does not lie in the central position.

Total energies for each chain are approximately invariant for each conformer. Correlation effects, incorporated approximately in the second order many-body perturbation theory results, do not alter this conclusion. Energy differences between conformers are less than 1 mhartree and are therefore insignificant, given the assumptions of this model. These results support previous conclusions on the approximate energetic equivalence of trans and gauche isomers.[11,22] There is no discernible trend with respect to chain length in the trans–gauche isomerization energies.

Electron binding energies, by contrast, vary significantly with respect to conformation. In odd Si chains, EPT(P4) ionization energies increase by about 0.3 eV and electron affinities are about 0.3 eV more negative. (On the uncorrelated level, the gap between the energies of the highest occupied and lowest unoccupied orbitals increases.) Similar changes occur for even chains where rotation occurs in the central Si-Si bond (Si_8H_{18} 4–5 and $Si_{10}H_{22}$ 5–6). The signs of the shifts are the same for the asymmetric even chains, but the magnitudes are closer to 0.2 eV.

FDAs for the all-trans $Si_{10}H_{22}$ chain are shown in Figures 1 and 2, for the ionization energy and the electron affinity, respectively. Note that the abscissa and ordinate have different scales (in Å) in order to display phase structure.

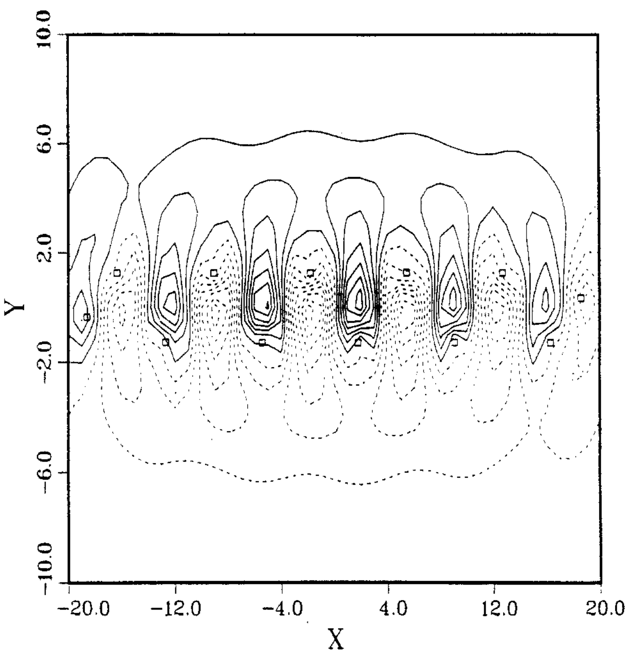

Figure 2. Feynman–Dyson amplitude for the electron affinity of $Si_{10}H_{22}$.

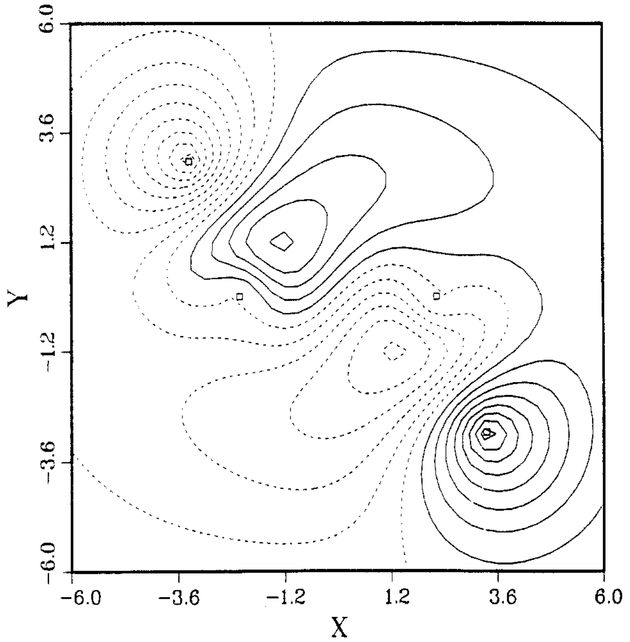

Figure 3. Feynman–Dyson amplitude for the electron affinity of distorted Si_2H_6.

Squares label positions of the ten Si and two terminal H nuclei. Solid (dashed) lines label positive (negative) contours in increments of 0.01; dashed lines also label nodes. Because of the use of the diagonal self-energy matrix approximation, these FDAs are equal to canonical orbitals. For the ionization energy case, one sees a pattern of Si–Si σ bond functions with alternating signs. This is a common feature of all polysilane oligomers and has been obtained in previous work on shorter chains[11,13-15] and on the top of the valence band of the infinite polymer.[22,23] In the latter limit, the orbital in question is constructed from Si p orbitals aligned with the chain axis and interfering constructively with their nearest neighbors.

For the electron affinity case, there is another repeating pattern that involves a localized function. This function, depicted in Figure 3, is the electron affinity FDA for a distorted Si_2H_6, where two elongated Si–H bonds that are trans with respect to each other produce a species with

Table III. Ionization Energy FDA Populations

molecule	1	2	3	4	5	6	7	8	9	10
Si_6H_{14}	0.093	0.169	0.211	0.211	0.169	0.093				
Si_7H_{16}	0.071	0.132	0.179	0.194	0.179	0.132	0.071			
	0.047	0.071	0.183*	0.216*	0.180	0.156	0.090			
Si_8H_{18}	0.055	0.106	0.149	0.175	0.175	0.149	0.106	0.055		
	0.058	0.104	0.121	0.192*	0.192*	0.121	0.104	0.058		
	0.026	0.038	0.132*	0.180*	0.182	0.180	0.141	0.076		
Si_9H_{20}	0.044	0.085	0.125	0.152	0.165	0.152	0.125	0.085	0.044	
	0.034	0.061	0.072	0.151*	0.177*	0.149	0.146	0.111	0.059	
$Si_{10}H_{22}$	0.035	0.069	0.104	0.132	0.150	0.150	0.132	0.104	0.069	0.035
	0.040	0.076	0.102	0.106	0.158*	0.158*	0.106	0.102	0.076	0.040
	0.019	0.036	0.042	0.114*	0.148*	0.151	0.159	0.142	0.102	0.054

Table IV. Electron Affinity FDA Populations

molecule	1	2	3	4	5	6	7	8	9	10
Si_6H_{14}	0.125	0.159	0.195	0.195	0.159	0.125				
Si_7H_{16}	0.071	0.132	0.179	0.194	0.179	0.132	0.071			
	0.038	0.004	0.207*	0.220*	0.151	0.174	0.151			
Si_8H_{18}	0.077	0.106	0.143	0.162	0.162	0.143	0.106	0.077		
	0.098	0.112	0.062	0.211*	0.211*	0.062	0.112	0.098		
	0.019	−0.003	0.152*	0.175*	0.166	0.185	0.150	0.109		
Si_9H_{20}	0.062	0.087	0.122	0.143	0.151	0.143	0.122	0.087	0.062	
	0.041	0.050	0.009	0.165*	0.180*	0.132	0.165	0.134	0.090	
$Si_{10}H_{22}$	0.051	0.073	0.104	0.126	0.139	0.139	0.126	0.104	0.073	0.051
	0.050	0.088	0.109	0.064	0.172*	0.172*	0.064	0.109	0.088	0.050
	0.020	0.027	0.000	0.125*	0.145*	0.139	0.168	0.155	0.108	0.082

C_{2h} symmetry. This function has both π bonding and σ antibonding character between the Si's. (The distortion is needed to mix FDAs that display one or the other type of Si–Si interaction in the D_{3d} geometry of Si_2H_6.) Because of its resemblance to the symbol on (among many instances) the South Korean flag, this motif shall be called a Yin–Yang function. Calculations on smaller chains consistently produce electron affinity FDAs that consist of Yin–Yang functions arranged to maximize constructive interference about each Si.[15] This effect is illustrated in Figure 2. In the limit of an infinite chain,[23] Si sp hybrids perpendicular to the chain axis interfere destructively with their neighbors at the bottom of the conduction band.

Mulliken charges for the FDAs are listed in Tables 3 and 4. Because this analysis pertains only to FDAs, not to many-electron wavefunctions, the charges for a given case sum to unity when all atoms are taken into account. The top row labels Si atoms in each chain. Mulliken charges are not observables in any sense, but they are useful for identifying trends in similar calculations on related molecules. For this qualitative purpose, they are employed here. Asterisks mark those Si atoms that are sites of rotated bonds. For each molecule, the first row pertains to the trans chain and the last row belongs to an asymmetric isomer with a single rotated bond. For the even chains, the second row corresponds to the symmetric, rotated conformer.

Inspection of the first row for each molecule discloses that there is a maximum of electron probability in the middle of each chain. Terminal atoms contribute least to these FDAs. When a rotated bond is introduced, several things change. In the resulting symmetric chains (Si_8H_{18} 4–5 and $Si_{10}H_{22}$ 5–6), where a C_2 operation relates one side of the molecule to the other, there is a concentration of probability in the atoms pertaining to the rotated bond. In both ionization energy and electron affinity cases, Si atoms next to the rotated bond suffer the greatest probability depletion. In the remaining chains with gauche defects, there is a similar concentration toward atoms of the rotated bond for electron affinity FDAs. For ionization energies, the trends are not as simple. The most obvious change for asymmetric chains is the probability reduction that occurs in atoms lying in the shorter of the two all-trans segments produced by the gauche defect. There is a concomitant increase in electron density in the longer of the two all-trans segments. For electron affinity FDAs, a local maximum of charge occurs near the middle of the longer trans segment. This also takes place for the ionization energy of $Si_{10}H_{22}$ 4–5.

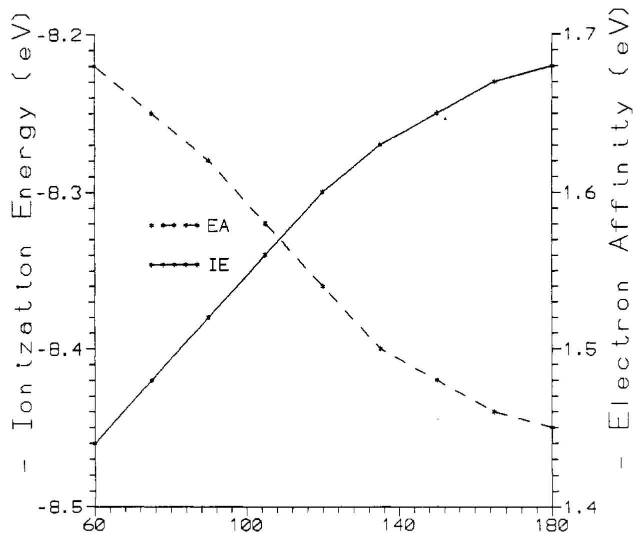

Figure 4. Ionization energy and electron affinity as a function of the 4–5 dihedral angle.

Detailed calculations on structures from all-trans $Si_{10}H_{22}$ to its 4–5 gauche defect isomer show how the electron binding energies and FDAs change with the dihedral angle.[43] A nondiagonal self-energy that includes infinite order ring and ladder improvements over partial fourth order is used for the all-trans and 4–5 structures. The differences between these results and second order results are the same for both structures. These differences are then added to second order results obtained for the intermediate structures. For small deviations from 180°, the changes in these energy differences are gradual. (See Figure 4.) The rate of change increases as the dihedral angle for the gauche isomer, 60°, is approached. Changes in the FDAs have a similar character. The sums of the

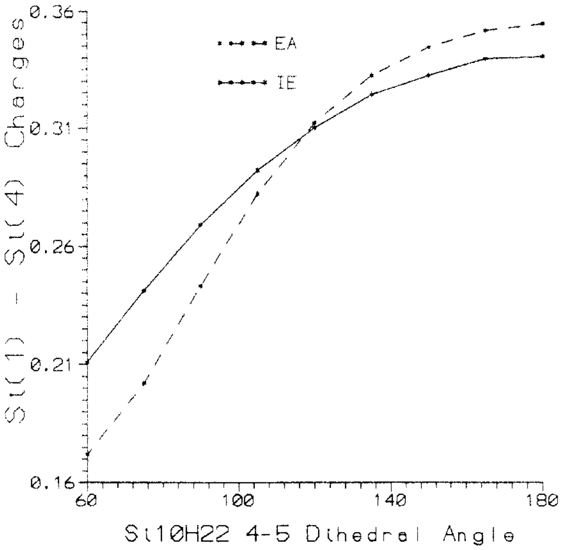

Figure 5. Sum of Mulliken charges for Si atoms 1 through 4 in ionization energy and electron affinity Feynman–Dyson amplitudes as a function of the 4–5 dihedral angle.

Mulliken charges for Si atoms 1 through 4 are displayed in Figure 5 as a function of dihedral angle. No abrupt changes take place when the all-trans structure is distorted.

Discussion

Previous investigations of smaller chains have shown how FDAs for ionization energies are built from Si–Si bonding lobes.[11–15] For the lowest ionization energy, the combination of bond functions displays alternating phases between neighbor functions. Electron affinity FDAs are built from Yin–Yang functions that are σ antibonding and π bonding between adjacent Si's. The largest electron affinity always corresponds to the most constructively interfering pattern possible. Interactions between contiguous two-center functions suffice to explain these generalizations about all-trans chains.

When considering the effects of dihedral angles, it is necessary to introduce first non-neighbor interactions to explain trends in electron binding energies. Changing a conformation from trans to gauche does not affect optimized Si–Si–Si bond angles or Si–Si bond lengths to an appreciable extent.[11] The explanation for the increase in the ionization energy lies in the in-phase first-non-neighbor interactions that are strengthened in the gauche conformation. For the ionization energy FDA, the phase relationship between these bond functions is always positive. In the gauche conformation, they are brought closer together, leading to an energy stabilization. Examination of kinetic energy contributions to correlated ionization energies confirms this explanation. When gauche defects are introduced, FDA kinetic energies decline by 0.4 eV for odd chains and symmetric even chains and by 0.3 eV for asymmetric even chains. Clearly, phase matching is controlling the overall behavior of the ionization energies as a function of conformation. The opposite energetic trend obtains for anion states, where the decisive component of these electron binding energies is increased electron repulsion for gauche isomers. The larger the amplitudes of the bond functions around the rotated bond, the bigger these effects on ionization energies and electron affinities will be. Because the largest amplitudes are found in the middle of the all-trans chains, rotations near the center will produce the biggest shifts. This is why, for the molecules with an even number of Si atoms, the shifts from all-trans to symmetric chains with a gauche defect are larger than those from all-trans to asymmetric chains.

When a gauche defect is introduced in an otherwise trans chain, there is a concentration of probability in the FDA toward the rotated single bond and away from its nearest neighbors. Provided there are no symmetry restraints forcing an equal distribution of probability on either side of the defect, electronic charges accumulate on the longer of the two remaining all-trans segments. This effect obtains for ionization energy and electron affinity FDAs, and it occurs gradually as a function of the dihedral angle of the rotated bond. As the chains become longer, probability maxima appear in the middle of the longer all-trans segment, especially for electron affinity FDAs. This suggests that a gauche defect will produce FDAs that resemble those of shorter all-trans chains. While there is a rough similarity in the electron binding energies and FDAs of, for example, all-trans Si_7H_{16} and $Si_{10}H_{22}$ 4–5, it is likely that the lengths of the chains under study here are not sufficient to illustrate these effects to the fullest possible extent.

Conclusions

One-electron states associated with ionization energies and electron affinities of oligomer models of polysilanes can be employed to understand the conformational dependence of electronic structure. Forming the most antibonding combination of Si–Si σ bond functions suffices to approximately construct an FDA associated with the lowest ionization energy of a chain. In a similar fashion, the most bonding combination of Yin–Yang functions is a good qualitative description of an electron affinity FDA. Introduction of a rotated bond in the form of a gauche conformational defect activates a non-neighbor overlap that stabilizes the ionization energy FDA. Charge redistributions destabilize the electron affinity FDA. Because the amplitudes of the two-center localized functions are larger at the center of the chains, energy shifts accompanying bond rotations will be larger when the rotation takes place about a central bond. When there is a symmetry relationship between two resulting all-trans segments, the FDAs remain relatively unaffected. If the two segments are of unequal length, localization on the longer of the two takes place. There is no abrupt change in the energies or distributions of the FDAs when a slight deviation from an all-trans structure is introduced. As chains increase in size, these localized states begin to resemble their counterparts in shorter all-trans chains. Calculations that impose symmetry do not represent chromophores that are likely to occur in polysilanes, where rotations about Si–Si bonds produce all-trans segments of various lengths.

Low symmetry chains with gauche defects have localized one-electron states near the Fermi level, but this is not necessarily the only circumstance where localization can occur. Localization could be produced by the accumulation of many smaller dihedral angle changes.[44] This possibility is currently under study.

Acknowledgment. This work was partially supported by the National Science Foundation under Grant CHE-9101777 and by the Petroleum Research Fund under Grant 24512-AC6. Support from the Department of Energy is acknowledged as well.

References and Notes

(1) West, R. *J. Organomet. Chem.* **1986**, *300*, 327.
(2) Miller, R. D.; Michl, J. *Chem. Rev.* **1989**, *89*, 1359.

(3) Pitt, C. G. In *Homoatomic Rings, Chains and Macromolecules of the Main Group Elements*; Rheingold, A. L., Ed.; Elsevier: New York, 1977.
(4) Harrah, L. A.; Zeigler, J. M. *J. Polym. Sci., Polym. Lett.* **1985**, *23*, 209. Trefonas, P., III; Damewood, J. R.; West, R. *Organometallics* **1985**, *4*, 1318. Miller, R. D.; Hofer, D.; Rabolt, J. F.; Fickes, G. N. *J. Am. Chem. Soc.* **1985**, *107*, 2172.
(5) Shukla, P.; Cotts, P. M.; Miller, R. D.; Russell, T. P.; Smith, B. A.; Walraff, G. M.; Baier, M.; Thiyagarajan, P. *Macromolecules* **1991**, *24*, 5606.
(6) Song, K.; Miller, R. D.; Walraff, G. M.; Rabolt, J. F. *Macromolecules* **1991**, *24*, 4084. Song, K.; Kuzmany, H.; Walraff, G. M.; Miller, R. D.; Rabolt, J. F. *Macromolecules* **1990**, *23*, 3870. Schilling, F. C.; Bovey, F. A.; Davies, D. D.; Lovinger, A. J.; Macgregor, R. B.; Walsh, C. A.; Zeigler, J. M. *Macromolecules* **1989**, *22*, 4645.
(7) Trefonas, P., III; West, R.; Miller, R. D. *J. Am. Chem. Soc.* **1985**, *107*, 2737. McKinley, A. J.; Karatsu, T.; Walraff, G. M.; Miller, R. D.; Sooriyakumaran, R.; Michl, J. *Organometallics* **1988**, *7*, 2567. Karatsu, T.; Miller, R. D.; Sooriyakumaran, R.; Michl, J. *J. Am. Chem. Soc.* **1989**, *111*, 1140.
(8) Kepler, R. G.; Zeigler, J. M.; Harrah, L. A.; Kurtz, S. R. *Phys. Rev. B* **1987**, *35*, 2818. Fujino, M. *Chem. Phys. Lett.* **1987**, *136*, 451.
(9) Hofer, D. C.; Miller, R. D.; Willson, C. G.; Neurather, A. *Proc. SPIE—Int. Soc. Opt. Eng.* (Advances in Resist Technology) **1984**, *469*, 108. Zeigler, J. M.; Harrah, L. A.; Johnson, A. W. *Proc. SPIE—Int. Soc. Opt. Eng.* (Advances in Resist Technology) **1985**, *539*, 166.
(10) West, R. In *Ultrastructure Processing of Ceramics, Glasses and Composites*; Hench, L., Ulrich, D. L., Eds.; John Wiley and Sons: New York, 1984.
(11) Ortiz, J. V.; Mintmire, J. W. *J. Am. Chem. Soc.* **1988**, *110*, 4522.
(12) Ortiz, J. V.; Mintmire, J. W. *Adv. Chem. Ser.* **1990**, *224*, 543. Mintmire, J. W.; Ortiz, J. V. In *Advances in Chemistry Series*; Zeigler, J. M., Gordon Fearon, F. W., Eds.; American Chemical Society: Washington, DC, 1990; Vol. 224, p 551.
(13) Ortiz, J. V.; Mintmire, J. W. *J. Phys. Chem.* **1991**, *95*, 8609.
(14) Ortiz, J. V. *J. Chem. Phys.* **1991**, *94*, 6064.
(15) Ortiz, J. V. *Polyhedron* **1991**, *10*, 1285.
(16) Nelson, J. T.; Pietro, W. J. *J. Phys. Chem.* **1988**, *92*, 1365.
(17) Cui, C. X.; Kertesz, M. *Macromolecules* **1992**, *25*, 1103.
(18) Bigelow, R. W.; McGrane, K. M. *J. Polym. Sci. B* **1986**, *24*, 1233.
(19) Crespo, R.; Piqueras, M. C.; Orti, E.; Bredas, J. L. *Synth. Met.* **1991**, *42*, 3457.
(20) Jalali-Heravi, M.; McManus, S. P.; Zutaut, S. E.; McDonald, J. K. *Chem. Mater.* **1991**, *3*, 1024.
(21) Kirtman, B.; Hasan, M. *J. Chem. Phys.* **1992**, *96*, 470.
(22) Mintmire, J. W.; Ortiz, J. V. *Macromolecules* **1988**, *21*, 1189.
(23) Mintmire, J. W. *Phys. Rev. B* **1989**, *39*, 13350. Mintmire, J. W. *Mater. Res. Soc.* **1989**, *141*, 235.
(24) Cui, C. X.; Karpfen, A.; Kertesz, M. *Macromolecules* **1990**, *23*, 3302.
(25) Teramae, H.; Takeda, K. *J. Am. Chem. Soc.* **19** , *111*, 1281. Teramae, H. *J. Am. Chem. Soc.* **1987**, *109*, 4140. Takeda, K.; Teramae, H.; Matsumoto, N. *J. Am. Chem. Soc.* **1986**, *108*, 8186.
(26) Orti, E.; Crespo, R.; Piqueras, M. C. *Synth. Met.* **1991**, *42*, 1575.
(27) Klingensmith, K. A.; Downing, J. W.; Miller, R. D.; Michl, J. *J. Am. Chem. Soc.* **1986**, *108*, 7438.
(28) Balaji, V.; Michl, J. *Polyhedron* **1991**, *10*, 1265.
(29) Schweizer, K. S. *J. Chem. Phys.* **1986**, *85*, 1156, 1176, 4181. Schweizer, K. S. *Chem. Phys. Lett.* **1986**, *125*, 118.
(30) Sun, Y. P.; Hamada, Y.; Huang, L. M.; Maxka, J.; Hsiao, J. S.; West, R.; Michl, J. *J. Am. Chem. Soc.* **1992**, *114*, 6301.
(31) Thorne, J. R. G.; Williams, S. A.; Hochstrasser, R. M.; Fagan, P. J. *Chem. Phys.* **1991**, *157*, 401.
(32) Thorne, J. R. G.; Repinec, S. T.; Abrash, S. A.; Zeigler, J. M.; Hochstrasser, R. M. *Chem. Phys.* **1990**, *146*, 315.
(33) Matsumoto, N.; Teramae, H. *J. Am. Chem. Soc.* **1991**, *113*, 4481.
(34) Frisch, M. J.; Head-Gordon, M.; Trucks, G. W.; Foresman, J. B.; Schlegel, H. B.; Ragavachari, K.; Robb, M. A.; Binkley, J. S.; Gonzalez, C.; DeFrees, D. J.; Fox, D. J.; Whiteside, R. A.; Seeger, R.; Melius, C. F.; Baker, J.; Martin, R. L.; Kahn, L.; Stewart, J. J. P.; Topiol, S.; Pople, J. A. *Gaussian 90*; Gaussian, Inc.: Pittsburgh, PA, 1990.
(35) EPT90, an electron propagator program by J. V. Ortiz, University of New Mexico.
(36) Bartlett, R. *Ann. Rev. Phys. Chem.* **1981**, *32*, 359. Binkley, J. S.; Pople, J. A. *Int. J. Quantum Chem.* **1975**, *9*, 229.
(37) Wadt, W. R.; Hay, P. J. *J. Chem. Phys.* **1985**, *82*, 284.
(38) Dunning, T. H.; Hay, P. J. In *Modern Theoretical Chemistry*; Schaefer, H. F., Ed.; Plenum: New York, 1976; Vol. 3.
(39) Linderberg, J.; Öhrn, Y. *Propagators in Quantum Chemistry*; Academic Press: New York, 1973. von Niessen, W.; Schirmer, J.; Cederbaum, L. S. *Comput. Phys. Rep.* **1984**, *1*, 57. Simons, J. *Theor. Chem. Adv. Persp.* **1978**, *3*. Herman, M. F.; Freed, K. F.; Yeager, D. L. *Adv. Chem. Phys.* **1981**, *48*, 1. Öhrn, Y.; Born, G. *Adv. Quantum Chem.* **1981**, *13*, 1.
(40) Koopmans, T. *Physica* **1933**, *1*, 104.
(41) Ortiz, J. V. *Int. J. Quantum Chem., Quantum Chem. Symp.* **1988**, *22*, 431. Ortiz, J. V. *J. Chem. Phys.* **1988**, *89*, 6348.
(42) Bock, H.; Ensslin, W.; Feher, F.; Freund, R. *J. Am. Chem. Soc.* **1976**, *98*, 668.
(43) Ortiz, J. V. *Macromolecules* **1993**, *26*, 2989.
(44) Tilgner, A.; Trommsdorff, H. P.; Zeigler, J. M.; Hochstrasser, R. M. *J. Chem. Phys.* **1992**, *96*, 781.